Muscarinic receptors induce LTD of NMDAR-EPSCs via a mechanism involving hippocalcin, AP2 and PSD-95

Kwangwook Cho, Jihoon Jo, Gi Hoon Son, Bryony Laura Winters, Myungjong Kim, Daniel Whitcomb, Bryony Dickinson, Youn-Bok Lee, Kensuke Futai, Mascia Amici, et al.

Muscarinic receptors induce LTD of NMDAR-EPSCs via a mechanism involving hippocalcin, AP2 and PSD-95

Jihoon Jo[1,4], Gi Hoon Son[1,4], Bryony L. Winters[1,2], Myung Jong Kim[3], Daniel J. Whitcomb[1], Bryony A. Dickinson[1], Youn-Bok Lee[1], Kensuke Futai[3], Mascia Amici[1,2], Morgan Sheng[3], Graham L. Collingridge[2] and Kwangwook Cho[1,2,CA]

[1]Henry Wellcome Laboratories for Integrative Neuroscience and Endocrinology (LINE), Faculty of Medicine and Dentistry, University of Bristol, Whitson Street, Bristol BS1 3NY, United Kingdom, [2]MRC Centre for Synaptic Plasticity, Department of Anatomy, University of Bristol, University Walk, Bristol BS8 1TD, United Kingdom, [3]The Picower Institute for Learning and Memory, Massachusetts Institute of Technology, Cambridge, MA 02139, USA.

[4] These authors contributed equally

[CA] Corresponding author: Dr. Kwangwook Cho, Henry Wellcome Laboratories for Integrative Neuroscience and Endocrinology, Faculty of Medicine & Dentistry, University of Bristol, Bristol BS1 3NY, United Kingdom. E-mail: Kei.Cho@bristol.ac.uk

Abstract

Although muscarinic acetylcholine receptors (mAChRs) and N-methyl-D-aspartate receptors (NMDARs) are of critical importance in synaptic plasticity, learning and memory, how they interact is poorly understood. We show that stimulation of muscarinic receptors, either by an agonist or by the synaptic release of acetylcholine, leads to long-term depression (LTD) of NMDAR-mediated synaptic transmission. This novel form of LTD involves the release of Ca^{2+} from IP_3-sensitive intracellular stores and is expressed via the internalisation of NMDARs. We present evidence that the molecular mechanism involves a dynamic interaction between the neuronal calcium sensor protein hippocalcin, the clathrin adaptor molecule AP2, the postsynaptic density enriched protein PSD-95 and NMDARs. We propose that under basal conditions hippocalcin binds to the SH3 region of PSD-95 but on sensing Ca^{2+} it translocates to the plasma membrane; in doing so it causes PSD-95 to dissociate from NMDARs so permitting AP2 to bind and initiate their dynamin-dependent endocytosis.

Introduction

It is well established that NMDARs are important triggers for the induction of both long-term potentiation (LTP)[1-3] and long-term depression (LTD)[4-7]. These two forms of synaptic plasticity involve alterations in the excitatory postsynaptic current (EPSC) that is mediated via the activation α-amino-3-hydroxy-5-methyl-4-isoxazole propionic acid receptors (AMPARs). In addition, it is now clear that NMDAR-mediated LTP and LTD also involve alterations in NMDAR-mediated EPSCs[8]. These alterations in NMDAR-mediated synaptic transmission will affect the ability of synapses to undergo subsequent synaptic plasticity and so represents a key form of metaplasticity[9]. The mechanism by which the synaptic activation of NMDARs results in LTP and LTD of AMPAR and NMDAR-mediated synaptic transmission is only partially understood, though a major component appears to involve alterations in the trafficking of these receptors to and from synapses[10].

The molecular processes that couple NMDAR activation to alterations in the synaptic expression of AMPARs and NMDARs are probably best understood for LTD of AMPAR-mediated synaptic transmission (NMDAR-LTD_A) in the hippocampus[7]. This process is triggered by a protein phosphatase cascade, involving PP2B and PP1[11,12], and also involves activation of kinases, such as glycogen synthase kinase-3[13,14], the membrane targeting of the high affinity neuronal calcium sensor (NCS) protein hippocalcin[15] and alterations in MAGUK proteins, in particular PSD-95[16,17].

The activation of muscarinic receptors may also be important for synaptic plasticity. It has been shown that pharmacological activation of these receptors can potentiate the activation of NMDARs[18, 19] and can facilitate the induction of NMDAR-LTP[20]. In addition, activation of muscarinic receptors can both facilitate the induction of NMDAR-LTD[21] and can induce an NMDAR-independent form of LTD[22]. However, most of the previous studies have activated muscarinic receptors by applying an agonist, such as carbachol (CCh), with very few investigations of how, or indeed whether, the synaptic release of ACh can influence synaptic plasticity via the activation of muscarinic receptors[23].

We have identified a new, direct and powerful interaction between NMDA and mACh receptor systems. We find that the activation of mAChRs induces LTD of NMDAR-mediated synaptic transmission (termed mAChR-LTD_N) by causing a dynamin-dependent internalisation of NMDARs. This process can be readily triggered by application of a muscarinic agonist or by the synaptic release of acetylcholine (Ach). It involves a novel signalling cascade in which the stimulation of muscarinic receptors results in IP_3-mediated Ca^{2+} release from intracellular stores, activation of hippocalcin and alterations in the association of AP2 and PSD-95 with NMDARs.

Results

Carbachol induces LTD on NMDAR-mediated synaptic transmission

Unless otherwise stated, all experiments were performed on acutely prepared rat hippocampal slices. NMDAR-mediated EPSCs ($EPSC_N$) were evoked by stimulation of Schaffer collateral-commissural fibres and recorded from CA1 neurons, held at -40 mV, following blockade of AMPAR- and GABAR-mediated responses. Bath application of CCh (50 μM, 10 min) induced LTD of $EPSC_N$ (61 ± 5 % of baseline measured 36 min after the end of the application, n = 6, filled symbols, **Fig. 1a**). Application of the M1 selective muscarinic antagonist pirenzepine (0.5 μM) eliminated this LTD (97 ± 4 %, n = 7, $p < 0.01$ *vs* control LTD, open symbols, **Fig. 1a**) leaving a reversible depression, which was presumably due to activation of a different muscarinic receptor subtype[24]. An M1 selective agonist (77-LH-28-1; 10 μM) induced a similar long-lasting depression, without inducing the transient depression, and its effects were eliminated by pirenzepine (77-LH-28-1: 64 ± 6 %, n = 6, filled symbols; pirenzepine: 95 ± 6 %, n = 6, open symbols, **Fig. 1b**). These results show that activation of

muscarinic receptors can induce LTD of $EPSC_N$ that is dependent on the activation of M1 receptors.

The mechanism of this novel form of LTD, termed CCh-LTD_N, was explored by introducing various agents into the recorded neuron using the patch pipette (**Fig. 1c-h**). None of the agents used affected basal NMDAR-mediated synaptic transmission or input resistance (data not shown). We found that CCh-LTD_N requires postsynaptic Ca^{2+} as it was inhibited by BAPTA (92 ± 4 %, n = 6; **Fig. 1c**). Since M1 receptors couple to the phosphoinositide pathway, it is likely that the Ca^{2+} source is IP_3-triggered Ca^{2+} release from intracellular stores. Consistent with an involvement of this canonical signalling pathway, LTD was blocked by 10 μM ryanodine (98 ± 3 %, n = 6; **Fig. 1d**) and an IP_3 receptor antagonist 2-aminoethoxydiphenyl borate (2-APB; 10 μM) (97 ± 3 %, n = 6, **Fig. 1e**). The other limb of the phosphoinositide pathway does not seem to be required, however, since a PKC inhibitor, that effectively blocks mGluR-LTD[25], was without effect (10 μM Ro 32-0432: 64 ± 4 %, n = 5; **Fig. 1f**). Since the prototypic form of LTD, induced by the activation of NMDARs, involves activation of the protein phosphatases PP1 and PP2B[11], we also tested inhibitors of these proteins, but found no effect (100 nM okadaic acid: 62 ± 6 %, n = 5, **Fig. 1g**; 10 μM ciclosporin 63 ± 4 %, n = 5; **Fig. 1h**). These results show that CCh-LTD_N involves IP_3-mediated release of Ca^{2+} from intracellular stores that then activates a non-classical mechanism.

LTD_N can be induced via the synaptic activation of mAChRs

Although the stimulation of muscarinic receptors using an agonist is useful for performing biochemical experiments and is relevant to how these cholinergic agents may act in the brain when administered therapeutically, the physiological relevance of such plasticity is questionable. We therefore investigated whether LTD_N could be induced by the synaptic activation of muscarinic receptors. We delivered paired-pulse low frequency stimulation (PP-LFS; 200 paired-pulses (50 ms interval) at 1 Hz)[26], in an attempt to activate the cholinergic fibres present in acute hippocampal slices, and held neurons at -40 mV so that we could simultaneously measure both fast component of EPSC ($EPSC_F$) and tail component of EPSC ($EPSC_T$) (**Fig. 2a, b**). Synaptic activation induced both LTD_F (filled circles: 63 ± 4 %, n = 6, **Fig. 2a**) and LTD_T (filled circles: 68 ± 4 %, n = 6, **Fig. 2b**), the induction of which was blocked by the addition of pizenzepine ($EPSC_F$: 105 ± 3 %, n = 6, Fig. 2a; $EPSC_T$: 111 ± 9 %, n = 6, **Fig. 2b**) or telenzepine ($EPSC_F$: 100 ± 7 %, n = 6, **Fig. 2a**; $EPSC_T$: 105 ± 5 %, n = 6, **Fig. 2b**).

Since there is inevitably some temporal overlap between $EPSC_A$ and $EPSC_N$ we performed all subsequent experiments after blocking AMPARs using NBQX. Since the synaptic activation of group I mGluRs can potentially induce LTD of NMDAR-mediated synaptic transmission[27,28] we also routinely blocked group I mGluRs by continuous perfusion of YM 298198 and 2-methyl-6-(phenylethynyl)-pyridine (MPEP) to eliminate the activation of $mGlu_1$ and $mGlu_5$ receptors, respectively. We then applied D-2-amino-5-phosphonopentanoate (D-AP5) to inhibit NMDARs and, whilst synaptic transmission was fully blocked, we delivered paired-pulse low frequency stimulation (**Fig. 2c-h**). This strategy was successful in activating a synaptic form of AChR-LTD_N since following washout of AP5 there was an LTD that was specific to the conditioned input (PP-LFS input: 69 ± 4 %, control input: 101 ± 4 %, n = 5; **Fig 2c**). This synaptically-induced LTD of $EPSC_N$ was similar in appearance to that induced by CCh and was prevented by the addition of pizenzepine (95 ± 6 %, n = 5; **Fig 2d**). Therefore it is possible to induce a robust LTD_N by the synaptic activation of muscarinic receptors (termed, syn-mAChR-LTD_N). Similar to CCh-LTD_N, syn-mAChR-LTD_N was also blocked by inclusion in the patch pipette of BAPTA (102 ± 8 %, n = 6; **Fig 2e**), ryanodine (98 ± 6 %, n = 6; **Fig 2f**) and 2-APB (98 ± 5 %, n = 6; **Fig 2g**) but not Ro-32-0432 (73 ± 4 %, n = 6; **Fig 2h**).

Hippocalcin is involved in CCh- and syn-mAChR-LTD_N

Having established that both CCh-LTD_N and syn-mAChR-LTD_N are dependent on postsynaptic Ca^{2+}, we wished to determine the nature of the Ca^{2+}-sensitive steps involved (**Fig. 3**). Since a key calcium sensor involved in synaptic plasticity is calmodulin, we tested a peptide inhibitor of this protein based on the calmodulin binding domain of myosin light chain kinase (MLCK; 10 μM) (**Fig. 3a-c**), which effectively blocks NMDAR-dependent LTD in the perirhinal cortex[25]. However, this MLCK peptide had no effect on either CCh-LTD_N (65 ± 3 %, n = 5, **Fig. 3a)** or syn-mAChR-LTD_N **(**64 ± 5 %, n = 6; **Fig. 3b**), though it did block NMDAR-LTD_A (**Fig. 3c**). Another Ca^{2+}-sensitive protein that has been shown to be involved in synaptic plasticity is hippocalcin[15], a member of the NCS family that is highly expressed in the hippocampus[29]. The role of hippocalcin can be explored using a well characterised dominant negative (GST-Hip_{2-72}), which is an N-terminal truncation that lacks the Ca^{2+} binding sites[15]. As shown in **Fig. 3(d-h)**, this treatment selectively blocked mAChR-LTD_N. Thus, postsynaptic infusion of GST-Hip_{2-72} blocks CCh-LTD_N, whilst in interleaved experiments GST alone had no effect (40 nM GST-Hip_{2-72}: 104 ± 3 %, n = 5; 40 nM GST: 63 ± 7 %, n = 5, $p<0.05$, **Fig. 3e**). Similarly, GST-Hip_{2-72} blocks syn-mAChR-LTD_N but GST

alone had no effect (GST-Hip$_{2-72}$: 99 ± 9 %, n = 5; GST: 62 ± 5 %, n = 5; **Fig 3f**). The effect of GST-Hip$_{2-72}$ was due to blockade of the induction of LTD$_N$ rather than by occlusion of the process, since baseline transmission was not affected (97 ± 10 %, n = 5, **Fig. 3d**). The effect was also selective for NMDARs since GST-Hip$_{2-72}$ had no effect on mAChR-LTD$_A$ induced by either CCh (66 ± 4 %, n = 5, **Fig. 3g**) or synaptic stimulation (66 ± 5 %, n = 5, **Fig. 3h**). These results demonstrate that hippocalcin is required for the LTD$_N$ that can be induced by the activation of muscarinic receptors.

Although the GST-Hip$_{2-72}$ dominant negative is an established tool for investigating the function of hippocalcin, it could have other actions. We therefore complemented this study by using a previously characterised RNAi probe that efficiently knocks down the expression of hippocalcin[25]. We generated hippocalcin-RNA interference (Hip-RNAi) constructs and tested their efficacy in cultured hippocampal neurons by immunocytochemistry. Hip-RNAi greatly suppressed the expression of hippocalcin whereas luciferase-RNAi had no effect (**Fig. 4a**). As a control, we tested the effects of Hip-RNAi on a different protein that is expressed in dendritic spines. We found that Hip-RNAi had no effect on the expression of PSD-95 (**Fig. 4b**).

We then studied synaptic function in organotypic slice cultures (**Fig. 4c-f**). To investigate the effects of hippocalcin knockdown on synaptic transmission, simultaneous recordings of EPSCs were performed from Hip-RNAi transfected and neighboring untransfected neurons. Hip-RNAi caused a small reduction of EPSC$_N$ but there were no significant differences in EPSC$_A$ between Hip-RNAi transfected cells and neighbouring untransfected cells (EPSC$_N$ in transfected cells, 222 ± 17 pA; EPSC$_N$ in untransfected cells, 286 ± 14 pA, n = 20 pairs, $p < 0.01$; EPSC$_A$ in transfected cells, 177 ± 15 pA; EPSC$_A$ in untransfected cells, 192 ± 18 pA, n = 20 pairs, $p > 0.05$; **Fig. 4c**). We next investigated whether Hip-RNAi had any effect on CCh-LTD$_N$. Consistent with the GST-Hip$_{2-72}$ experiments, transfection of Hip-RNAi blocked CCh-LTD$_N$, whereas CCh-LTD$_N$ was routinely induced in simultaneously recorded, neighbouring untransfected cells (Hip-RNAi: 99 ± 9 %, n = 5; untransfected: 63 ± 4 %, n = 5, $p < 0.05$; **Fig. 4d**). We confirmed that CCh-LTD$_N$ in organotypic slices was likely to be the same form of synaptic plasticity as CCh-LTD$_N$ in acute slices by demonstrating sensitivity to pirenzepine (96 ± 8 %, n = 6, **Fig. 4e**). Consistent with the lack of effect of Hip$_{2-72}$ on mAChR-LTD$_A$, Hip-RNAi had no effect on CCh-LTD$_A$ (62 ± 3 %, n = 6, $p > 0.05$ *vs* control; **Fig. 4f**) confirming the selective involvement of hippocalcin in LTD of NMDAR-mediated synaptic transmission when muscarinic receptors are activated.

mAChR-LTD$_N$ involves internalisation of NMDARs

The next question that we wanted to address is the locus of expression of mAChR-LTD$_N$. Since other forms of LTD involve the internalisation of receptors[10] we investigated whether CCh-LTD$_N$ might involve internalisation of NMDARs using surface biotinylation experiments. Hippocampal slices were treated with CCh (10 min), in the presence or absence of pirenzepine, and the cell surface and total expression levels of the GluN1 subunit of the NMDAR were compared (**Fig. 5a**). CCh reduced surface GluN1 (55 ± 1% of control, n = 4, $p < 0.05$ *vs* control) without affecting total expression of GluN1, in a pirenzepine-sensitive manner (121 ± 21 % of control, $p > 0.05$ *vs* control). If the internalisation of NMDARs is indeed the expression mechanism involved in mAChR-LTD$_N$ then preventing endocytosis should inhibit this form of LTD. Since most forms of receptor endocytosis that have been associated with LTD are dynamin-dependent, we used dynasore, an inhibitor of this process. Consistent with this idea, dynasore blocked both CCh-LTD$_N$ (98 ± 4 %, n = 6, **Fig. 5b)** and syn-mAChR-LTD$_N$ (102 ± 6 %, n = 5, **Fig. 5c**) in acute hippocampal slices.

mAChR-LTD$_N$ involves dynamic interactions between NMDARs, hippocalcin, AP2 and PSD-95

A robust biochemical correlate of mAChR-LTD$_N$ enabled us to explore the molecular mechanisms involved in more detail. Since hippocalcin interacts with the clathrin adaptor protein AP2[15] and since AP2 is involved in the internalisation of NMDARs, where it might compete with PSD-95[30], we investigated the interactions of these three molecules with NMDAR subunits, using co-immunoprecipitation (co-IP) assays (**Fig. 6a**). CCh increased the association between GluN1 and the β-adaptin subunit of AP2, whilst reducing the association between GluN1 and PSD-95. Hippocalcin co-immunoprecipitated with GluN1 and PSD-95 under basal conditions. CCh caused a substantial reduction in this association (**Fig. 6b**). Interestingly, CCh had no effect on the association between hippocalcin and β-adaptin (**Fig. 6c**). CCh also had no effects on protein expression levels of PSD-95, GluN1 and β-adaptin (**Fig. 6d**). These data indeed show that dynamic interactions occur between hippocalcin, AP2 and PSD-95 and that these interactions are associated with the internalisation of NMDARs that is triggered by the activation of muscarinic receptors. The results are consistent with a model in which hippocalcin promotes the exchange of AP2 for PSD-95 on NMDARs, thereby initiating this process.

To examine whether hippocalcin can directly interact with NR1 or PSD-95, we employed a mammalian two-hybrid assay system[31] (**Fig. 7a**, **b**). We prepared VP16AD-tagged constructs (AD) of c-terminal NMDAR (AD-GluN1ct), three PDZ domains of PSD-95 (AD-95PDZ) and the SH plus guanylate kinase-like (GK) domains of PSD-95 (AD-95SHGK) (**Fig. 7a**). Truncated hippocalcin was tagged with GAL4BD protein (BD-Hip_{2-72}, BD-$Hip_{104-192}$, **Fig. 7a**). Luciferase assays indicated that the N-terminal region of hippocalcin (Hip_{2-72}) strongly interacted with the SHGK domain and weakly interacted with the PDZ domain, whereas the c-terminal region of hippocalcin did not interact with either portion of PSD-95. Neither part of hippocalcin interacted with the c-terminal region of GluN1 (**Fig. 7b**). Consistent with mammalian two-hybrid experiments, GST pull-down assays also confirmed that Hip_{2-72} interacts with the SHGK domain of PSD-95 more strongly than the PDZ domain (**Fig. 7c**). In addition, Hip_{2-72} did not interact with SH deleted PSD-95 (95ΔSH3) but interacted with GK deleted PSD-95 (95ΔGK) (**Fig. 7d**). These results suggest that hippocalcin specifically interacts with the SH3 domain of PSD-95.

If this interaction has any functional significance it would be expected that the interaction might vary according to Ca^{2+} concentration, particularly over the nano-molar concentration range over which hippocalcin senses Ca^{2+}. Therefore, GST-hippocalcin pull-down assays were carried out using hippocampal lysates and a range of free [Ca^{2+}]. There was a strong association of hippocalcin with both PSD-95 and GluN1 at a free [Ca^{2+}] of 10^{-8} M. This association decreased dramatically over the concentration range (10^{-7} to 10^{-5} M) that hippocalcin senses Ca^{2+} (**Fig. 7e**). These data are consistent with hippocalcin decreasing its association with the NMDAR complex on sensing Ca^{2+}.

The SH-domain of PSD-95 is required for mAChR-LTD_N

To further determine the region of PSD-95 that is involved in the interaction and to establish the functional significance of this interaction, we used RNAi to knock down endogenous PSD-95 and co-expressed a variety of RNAi resistant PSD-95 constructs (PSD95 RNAiRs) using slice cultures (**Fig. 8**). In paired-cell recordings[25], transfection of PSD-95 RNAi (PSD95-RNAi) results in inhibition of $EPSC_N$ (PSD95-RNAi: 119 ± 13 pA, n = 20; untransfected cells: 274 ± 14 pA, n = 20, $p < 0.005$; **Fig. 8a** left) and $EPSC_A$ (PSD95-RNAi: 102 ± 12 pA, n = 20; untransfected cells: 273 ± 18 pA, n = 20, $p < 0.005$; **Fig. 8a** right) and completely prevents the induction of CCh-LTD_N (PSD95-RNAi: 101 ± 3 %; untransfected: 66 ± 5 %, n = 5, $p < 0.01$; **Fig. 8b**). Co-expression of an RNAi resistant form of full-length PSD-95 (PSD95 RNAiR) and PSD95-RNAi resulted in an increase in both $EPSC_N$ (PSD95

RNAiR: 240 ± 23 pA, n = 16; untransfected cells: 168 ± 11 pA, n = 16, p < 0.01; **Fig. 8c** left) and $EPSC_A$ (PSD95 RNAiR: 270 ± 26 pA, n = 18; untransfected cells: 153 ± 11 pA, n = 16, p < 0.01; **Fig. 8c** right). These results are consistent with the overexpression of PSD-95 reported in other studies[17,32-34]. In contrast, CCh-LTD_N was unaffected by this treatment (65 ± 3%, n = 5; **Fig. 8d**). Therefore, co-expression of PSD95 RNAiR enabled full rescue of the LTD deficit induced by knockdown of PSD-95.

Co-expression with an RNAi resistant form of GK deleted PSD-95 (ΔGKPSD95 RNAiR) and PSD95-RNAi had very similar effects. Thus, this treatment caused increases in basal $EPSC_N$ (ΔGKPSD95 RNAiR: 227 ± 16 pA, n = 14; untransfected cells: 178 ± 19 pA, n = 14, p < 0.05; **Fig. 8e** left) and $EPSC_A$ (ΔGKPSD95 RNAiR: 296 ± 20 pA, n = 14; untransfected cells: 192 ± 22 pA, n = 14, p<0.01; **Fig. 8e** right) and LTD_N was again rescued (ΔGKPSD95-RNAiR: 68 ± 5 %; untransfected: 67 ± 4 %, n = 5, p>0.05; **Fig. 8f**). In contrast, an RNAi resistant form of the SH-domain deleted PSD-95 (ΔSHPSD95 RNAiR) had very different effects. Whilst, like the other constructs, it increased AMPAR-mediated synaptic transmission (ΔSHPSD95 RNAiR: 256 ± 18 pA, n = 18; untransfected cells: 138 ± 17 pA, n = 18, p < 0.01; **Fig. 8g** right) it did not affect NMDAR-mediated synaptic transmission (ΔSHPSD95 RNAiR: 138 ± 18 pA, n = 18; untransfected cells: 145 ± 14 pA, n = 18, p > 0.05; **Fig. 8g** left). Significantly, it was unable to rescue the deficit in LTD_N (ΔSHPSD95 RNAiR: 96 ± 5 %; untransfected cells: 63 ± 4 %, n = 5, p<0.05; **Fig. 8h**). These experiments confirm and extend the biochemical studies by identifying the SH domain of PSD-95 as important for mAChR-LTD_N.

Discussion

Activation of mAChRs induces LTD of NMDAR-mediated synaptic transmission

It is well established that, like AMPAR-mediated synaptic transmission, NMDAR-mediated synaptic transmission is highly plastic and can readily undergo both LTP and LTD[35]. However, this plasticity is generally induced by the synaptic release of L-glutamate acting on ionotropic or metabotropic glutamate receptors. Our present finding that the synaptic activation of muscarinic receptors can readily induce LTD of NMDAR-mediated synaptic transmission adds a new dimension to the plastic capabilities of the brain

A role for hippocalcin in mAChR-LTD_N

A principal mechanistic finding of the present study is that hippocalcin is required for mAChR-LTD$_N$. Hippocalcin is uniquely suited to this role since it has a high affinity for Ca^{2+} and, unlike most of the other members of the NCS family, undergoes a conformational change on binding Ca^{2+} to expose its myristoylated region, which then leads to its targeting to the plasma membrane[29]. Interestingly, hippocalcin seems to use this unique property for several different neuronal functions. Thus, it has been found to play a role in the endocytosis of AMPARs following the stimulation of NMDARs[15] and in the Ca^{2+} activation of certain K^+ channels[36]. However, hippocalcin is not involved in all types of synaptic plasticity. For example, we show here that it does not mediate mAChR-LTD$_A$. This result, which at first might seem surprising in light of the role of hippocalcin in NMDAR-mediated LTD$_A$[15], is consistent with the finding that CCh-LTD$_A$ is a calcium-independent form of synaptic plasticity[22]. Therefore the involvement of hippocalcin neither correlates with the receptor involved in induction nor with the receptor involved in expression of synaptic plasticity. It clearly has a complex role depending on the form of plasticity, which presumably relates, at least in part, to the precise requirements for Ca^{2+} and perhaps the microdomains in which the different forms of synaptic plasticity operate. It is possible that mAChR-LTD$_N$ and NMDAR-LTD$_A$ operate in different types of spine, given that the former requires IP_3-mediated Ca^{2+} release from intracellular stores and that this apparatus might only exist in a subset of spines[37]. A potential mechanism that might explain the role of hippocalcin in mAChR-LTD$_N$ and NMDAR-LTD$_A$ is illustrated in **supplementary figure**.

The mechanism of expression of mAChR-LTD$_N$ appears to be the internalisation of NMDARs. This suggestion is supported by the finding that dynasore, which blocks dynamin-dependent internalisation[38], eliminates mAChR-LTD$_N$ and since carbachol treatment leads to an M1-dependent internalisation of NMDARs. It was already known that NMDARs can undergo clathrin-mediated endocytosis but the trigger for, and functional significance of, this process was unknown. Previous work has shown that PSD-95 and β-adaptin can bind to a similar region of the intracellular tail of GluN2B subunits and it was therefore suggested that the function of PSD-95 might be to inhibit clathrin-mediated endocytosis[30]. Here we provided further experimental support for this hypothesis and have identified a potential molecular mechanism. We suggest that Ca^{2+} release from intracellular stores, resulting from the stimulation of muscarinic receptors, triggers hippocalcin to initiate an exchange of β-adaptin for PSD-95 at NMDARs thereby initiating their endocytosis.

A role for PSD-95 in mAChR-LTD$_N$

Previous studies have shown that PSD-95 regulates NMDAR surface expression[30] and is involved in NMDAR-LTD_A[16,17,39,40]. In particular, this form of LTD requires dephosphorylation of ser295, a residue in a linker region between the PDZ domains 2 and 3[16]. It also involves interactions with the SH3/GK domain, where one function might be to associate with calcineurin, via an interaction with AKAP79/150, so that this enzyme is located close to NMDARs[17]. Our findings show that the involvement of PSD-95 is not restricted to this one form of LTD but rather it extends to LTD triggered via the activation of a G-protein-coupled receptor (in this case the muscarinic receptor) and expressed by changes in NMDAR-mediated synaptic transmission. Using a similar knockdown and replacement strategy to that employed previously[17], we identified that the SH3 domain of PSD-95 is involved in mAChR-LTD_N.

One possible mechanism that can explain our results is that under basal conditions, hippocalcin binds to the SH3 domain of PSD-95 (**supplementary figure**). On binding Ca^{2+}, hippocalcin translocates to the plasma membrane and in doing so permits the disassociation of PSD-95 from NMDARs. This would then enable AP2, which is itself targeted to the vicinity of the plasma membrane by hippocalcin, to bind NMDARs and initiate their endocytosis. Consistent with this model, the PSD-95 mutant that lacks the SH domain could still bind NMDARs but would not bind hippocalcin. Also consistent with this model, the hippocalcin dominant negative would block the process since this would bind to PSD-95 but would not dissociate in response to a rise in Ca^{2+}.

In addition to a role in LTD, it is well established that PSD-95 can regulate AMPAR mediated synaptic transmission by promoting insertion of AMPARs at synapses[32,41,42]. It has been suggested that this effect and the effect on LTD involves different interaction sites within PSD-95[17]. Our findings support the view that the functions of PSD-95 on baseline synaptic transmission and synaptic plasticity can be dissociated, since all three forms of PSD-95 that we expressed increased AMPAR-mediated synaptic transmission but only the SH3 mutant blocked mAChR-LTD_N. The effect of PSD-95 expression on NMDAR-mediated synaptic transmission is less clear, with reports of small increases[34] or no effect[17]. We observed a small increase in $EPSC_N$ with overexpression of wildtype PSD-95 and the PDZ domain mutant but no change with the SH3 mutant. This suggests that the effects on NMDAR-mediated synaptic transmission and synaptic plasticity of $EPSC_N$ might be related. For example, the inhibition of LTD over a period of a few days might have led to the small increase in synaptic transmission, a likely scenario if synaptic transmission in set by a balance

of ongoing LTP and LTD. However, the complete block of LTD cannot be attributed to the small increase in synaptic transmission. The most compelling evidence in support of this is that the dominant negative applied via the patch pipette eliminated LTD without affecting baseline transmission. These findings emphasise the importance of complementary strategies (in this case dominant negative and RNAi) to understand the functions of proteins in synaptic plasticity.

Concluding remarks

We have identified a new form of synaptic plasticity in which the activation of NMDARs can be depressed for long periods of time by the activation of muscarinic receptors. Our work has revealed a novel mechanism of synaptic plasticity involving the interplay between NMDARs, hippocalcin, AP2 and PSD-95.

ACKNOWLEDGMENTS

This work was funded by the BBSRC (K.C.), MRC (G.L.C.), UK Alzheimer's Research Trust (K.C., D.W.), The Royal Society (J.J.) and Brain Research Centre of the 21st Century Frontier Research Programme funded by the Korean Ministry of Education and Science and Technology (K.C. and G.L.C.).

AUTHORS CONTRIBUTIONS

The study was conceived by K.C., the experiments were designed by K.C. M.S. and G.L.C., carried out by J.J., G.H.S., B.L.W., M.J.K., D.J.W., B.A.D., Y.L., K.F. and M.A. and the manuscript was written by G.L.C., M.S. and K.C.

FIGURE LEGENDS

Fig. 1. Activation of muscarinic receptors induces LTD of NMDAR-mediated synaptic transmission. (a) Bath application of carbachol (CCh; 50 μM, 10 min, filled symbols) induces LTD of NMDAR-mediated EPSCs (LTD_N), which is prevented by pirenzepine (0.5 μM, open symbols). (b) An M1 selective agonist (77-LH-28-1; 10 μM, 10 min, filled symbols) induces LTD_N and this LTD is prevented by pirenzepine (open symbols). (c-e) Postsynaptic infusion of BAPTA (10 mM), ryanodine (10 μM) and 2-APB (10 μM) in the patch pipette blocks CCh-LTD_N. (f-h) Postsynaptic inclusion of Ro-32-0432 (10 μM), okadaic acid (100 nM) and ciclosporin (10 μM) in the patch pipette has no effect on CCh-LTD_N. In this and subsequent figures, error bars indicate mean ± SE mean.

Fig. 2. The synaptic activation of muscarinic receptors induces LTD_N. (a) Paired-pulse low frequency stimulation (PP-LFS) induces pirenzepine- and telenzepine-sensitive LTD in fast component of EPSC ($EPSC_F$). (b) Paired-pulse low frequency stimulation (PP-LFS) induces pirenzepine- and telenzepine-sensitive LTD in tail component of EPSC ($EPSC_T$). (c) Paired-pulse low frequency stimulation (PP-LFS) induces a pirenzepine-sensitive LTD of pure NMDAR-EPSCs (syn-mAChR-LTD_N). AP5 was applied to prevent the potential induction of NMDAR-LTD and the level of LTD was assessed following washout of the NMDAR antagonist. An $mGlu_1$ (YM 298198; 1 μM) and an $mGlu_5$ antagonist (MPEP; 10 μM) were applied throughout to prevent mGluR-LTD (filled symbols: LTD input; open symbols: control input). (d) Syn-mAChR-LTD_N is prevented by pirenzepine. (e-g) Postsynaptic inclusion in the patch pipette of BAPTA, ryanodine and 2-APB blocks syn-mAChR-LTD_N. (h) Postsynaptic inclusion of Ro-32-0432 in the patch pipette has no effect on syn-mAChR-LTD_N.

Fig. 3. Hippocalcin is required for mAChR-LTD_N. (a-c) Postsynaptic inclusion of a portion of myosin light chain kinase (MLCK; 10 μM), a calmodulin inhibitor, has no effect on (a) CCh-LTD_N and (b) syn-mAChR-LTD_N but (c) blocks NMDAR-LTD_A. (d-h) Effects of postsynaptic infusion of GST-Hip_{2-72}. (d) GST-Hip_{2-72} has no effect on basal NMDAR-mediated synaptic transmission. (e, f) GST-Hip_{2-72} (filled symbols) but not GST alone (open symbols) blocks CCh-LTD_N and syn-mAChR-LTD_N, respectively (g,h). GST-Hip_{2-72} has no effect on CCh-LTD_A or syn-mAChR-LTD_A, respectively.

Fig. 4. Hippocalcin-RNA interference (Hip-RNAi) blocks CCh-LTD_N. (a) Hip-RNAi inhibits expression of hippocalcin in cultured hippocampal neurons. (b) Hip-RNAi has no effect on the expression of PSD-95. (c) Pair-wise analysis of basal synaptic transmission between Hip-RNAi transfected neurons and untransfected neighbouring cells. Hip-RNAi transfection induces a moderate inhibition of $EPSC_N$ ($p < 0.05$, $n = 20$ pairs, left) but has no effect on $EPSC_A$ ($p > 0.05$, $n = 20$ pairs, right). (d) Simultaneous dual-patch recording from Hip-RNAi transfected and untransfected neighbouring cells. Hip-RNAi blocks CCh-LTD_N but untransfected neighbouring cells display normal CCh-LTD_N. (e) Pirenzepine prevents CCh-LTD_N in slice cultures. (f) Hip-RNAi has no effect on CCh-LTD_A.

Fig. 5. mAChR-LTD_N involves the internalisation of NMDARs. (a) Biotinylation assays show that CCh induces a reduction in surface but not total GluN1 expression, in a pirenzepine-sensitive manner. (b) Postsynaptic inclusion of dynasore blocks CCh-LTD_N ($n = 6$). (c) Postsynaptic inclusion of dynasore blocks syn-mAChR-LTD_N ($n = 6$).

Fig. 6. Dynamic interactions between NMDARs, hippocalcin, AP2 and PSD-95. (a) Co-IP assays show that CCh causes an increased association of β-adaptin and a decreased association of PSD-95 with NMDARs. The association of NR1 and NR2 subunits does not change. (b) Co-IP assays show that hippocalcin associates with the NMDAR complex and CCh causes its disassociation. (c) CCh has no effect on the association between hippocalcin and β-adaptin. CCh (50 μM) was applied to hippocampal slices for 10 min at $t = 0$. (d) CCh has no effect on the total protein expression levels of PSD-95, GluN1 and β-adaptin. Histograms plot the quantification from at least 3 independent experiments. *: $p < 0.05$, **: $p < 0.01$ *vs* control.

Fig. 7. Hippocalcin interacts with PSD-95. (a) Schematic representations of gene constructs for mammalian two-hybrid assay. (b) Protein interactions revealed by two-hybrid assay. -: no interaction; +: weak interaction (1.5 ~ 2 fold induction in luciferase reporter); +++: strong interaction (more than 3 fold induction). (c) GST-pull down assays show that Hip_{2-72} interacts with SHGK domains of PSD-95 more strongly than the PDZ domain of PSD-95. (d) GST pull-down indicates that Hip_{2-72} interacts with SH domain of PSD-95. (e) The interaction of hippocalcin with PSD-95 and GluN1 is Ca^{2+}-dependent. *: $p < 0.05$, **: $p < 0.01$ *vs* $10^{-8}[Ca^{2+}]_{free}$.

Fig 8. The SH domain of PSD-95 is involved in CCh-LTD_N. (a) Pair-wise analysis of basal synaptic transmission between neurons expressing PSD95-RNAi and untransfected neighbouring cells. PSD95-RNAi inhibits $EPSC_N$ ($p < 0.005$, $n = 20$) and $EPSC_A$ ($p < 0.005$, $n = 20$). (b) This construct also blocks CCh-LTD_N ($n = 5$). (c) Pair-wise analysis of basal synaptic transmission between co-transfection of PSD95-RNAi and RNAi-resistant PSD95 (PSD95 RNAiR) and untransfected neighbouring cells. PSD95 RNAiR enhances $EPSC_N$ ($p < 0.05$, $n = 16$) and $EPSC_A$ ($p < 0.05$, $n = 16$). (d) Co-transfection of PSD95-RNAi and PSD95 RNAiR has no effect on CCh-LTD_N ($n = 5$). (e) Equivalent experiments but using a GK domain of PDS-95 deleted RNAiR (ΔGKPSD95 RNAiR) produced similar effects on basal synaptic transmission; $EPSC_N$ ($p < 0.05$, $n = 18$) and $EPSC_A$ ($p < 0.05$, $n = 18$). (f) This construct also enabled CCh-LTD_N to be induced ($n = 5$). (g) When equivalent experiments were performed using an SH domain of PSD-95 deleted RNAiR (ΔSHPSD95 RNAiR) the effect on basal $EPSC_N$ ($p > 0.05$, $n = 18$) was no longer observed but the effect on $EPSC_A$ persisted ($p < 0.05$, $n = 18$). (h) This construct did not enable CCh-LTD_N to be induced in the transfected neurons ($n = 5$) but untransfected neighbouring cells displayed normal CCh-LTD_N ($n = 5$).

Methods

Electrophysiology. Hippocampal slices were obtained from 4-5 week old male Wistar rats. Animals were sacrificed by dislocation of the neck and decapitated, and the brain rapidly removed and placed in ice-cold artificial cerebrospinal fluid (aCSF; bubbled with 95% O_2/5% CO_2) containing the following: (in mM) NaCl, 124; KCl, 3; $NaHCO_3$, 26; NaH_2PO_4, 1.25; $CaCl_2$, 2; $MgSO_4$, 1; D-glucose, 10. Subsequently, a midsagittal cut was made to the brain and one hemisphere was placed back into the ice cold aCSF until it was required. Transverse hippocampal slices (400 μm) were prepared using a McIllwain tissue chopper (Mickle Laboratory Engineering Co. Ltd., Gomshall, UK). The slices were then carefully placed into a submersion chamber saturated with 95% O_2 / 5% CO_2, at room temperature (22 ~ 25°C) and left to recover for a minimum of 1 hour. For the recording, slices were transferred to the recording chamber, perfused with aCSF (28°C ~ 30°C, flow rate 2~3 ml/min). Before recording, the CA3 region of the hippocampus was severed using a scalpel cut to prevent epileptiform bursting.

Excitatory postsynaptic currents (EPSCs) were recorded using a Multiclamp 700B amplifier (Axon Instruments, Foster City, USA). Pipette solution was comprised of (mM): $CsMeSO_4$, 130; NaCl, 8; Mg-ATP, 4; Na-GTP, 0.3; EGTA, 0.5; HEPES, 10; QX-314, 6. The pH was adjusted to 7.2-7.3 using CsOH, while osmolarity was adjusted to 270-290 mOsm with sucrose as necessary. Electrodes were pulled using a horizontal Flaming Brown puller (P-97, Sutter Instruments Co, USA). Electrode resistance was in the range 4-6 MΩ. CA1 pyramidal neurons were voltage clamped at –40 mV and NMDA receptor current was measured in the presence of NBQX (5 μM) and picrotoxin (20 μM). In simultaneous measurement of fast and tail component of EPSCs, the peak currents were measured 10 - 15 ms and 50 - 60 ms after stimulation. Stimulating electrodes placed into the Schaffer collateral-commissural pathway in the CA2 region delivered stimuli at a frequency of 0.033 Hz. Series resistance and input resistance were monitored during the experiment and for inclusion in analysis, cells were required to have a series resistance (R_s) < 20 MΩ, where neither measurement changed by more than 10% during an experiment. The peak current amplitudes of NMDAR EPSCs were measured online using WinLTP software (http://www.ltp-program.com)[43].

In the whole cell patch recording experiments, a baseline of at least 10 minutes was obtained before application of CCh or PP-LFS. After drug application, a washout period of 40 minutes was obtained. BAPTA, okadaic acid, cyclosporin A, Ro 32-0432 and MLCK were added to the whole cell-patch filling solution. These chemicals were purchased from Calbiochem (San

Diego, CA, USA). AP-5, MPEP, NBQX, picrotoxin and YM 298198 were purchased from Ascent Scientific (Bristol, UK). Pirenzepine and CCh were purchased from Tocris (Bristol, UK). These chemicals were made up as a stock solution and diluted to their final appropriate concentration in ACSF as required.

Organotypic hippocampal slice culture. Organotypic hippocampal cultures were prepared according to the interface method[16]. Slices were prepared from postnatal days 6-7 Wistar rats. Rats were decapitated, and the brain was rapidly removed and placed in cold cutting solution that comprised: (in mM) Sucrose, 238; KCl, 2.5; $NaHCO_3$, 26; NaH_2PO_4, 1; $MgCl_2$, 5; D-glucose, 11; $CaCl_2$, 1. Hippocampus was dissected and transversely sliced at a thickness of 350 μm on a McIlwain tissue chopper, and placed on top of semipermeable membrane inserts (Millipore Corporation, Bedford, MA, USA) in a six-well plate containing culture medium (78.8% minimum essential medium, 20% heat-inactivated horse serum, 30 mM HEPES, 26 mM D-glucose, 5.8 mM $NaHCO_3$, 2 mM $CaCl_2$, 2 mM $MgSO_4$, 70 μM Ascorbic Acid, 1μg/ml Insulin, pH adjusted to 7.3 and 320-330 osmolarity). Slices were cultured in an incubator (35 C, 5% CO_2) for 14-16 days *in vitro* (DIV) with a change of medium every two days. No antibiotics were used. Neurons were transfected using a biolistic gene gun (BioRad, USA) at DIV 10-12 (100 μg DNA; 90% of the construct to test; 10% pEGFP-C1). Electrophysiological recordings were performed at 3–4 days after transfection. Recordings were carried out in solution containing (mM): NaCl 119, KCl 2.5, $CaCl_2$ 4, $MgCl_2$ 4, $NaHCO_3$ 26, NaH_2PO_4 1, glucose 11, picrotoxin 0.02, and 2-chloroadenosine 0.01, gassed with 5% CO_2/95% O_2, at pH 7.4. In some of experiments, dual patch recordings were made simultaneously from a pair of neighboring CA1 pyramidal neurons, one transfected and the other untransfected cell.

Hippocalcin RNAi. For the pSUPER-Hippocalcin-RNAi construct, the following oligonucleotides were annealed and inserted into the *Hin*dIII/*Bgl*II sites of pSUPER vector[44]. 5'- GAT CCC CGA AGA TCT ACG CCA ACT TCT TCA AGA GAG AAG TTG GCG TAG ATC TTC TTT TTA-3'; 5'- AGC TTA AAA AGA AGA TCT ACG CCA ACT TCT CTC TTG AAG AAG TTG GCG TAG ATC TTC GGG-3'.

PSD-95 constructs. The following PSD-95 constructs were subcloned into the pSUPER vector. PSD-95 RNAi: 5′-GCCTTCGACAGAGCCACGA-3′ RNAi resistance PSD-95 (PSD95-RNAiR): 5-GCGTTTGATAGGGCCACGA-3[34].

Antibodies and immunoblotting. Anti-hippocalcin antibody was described previously[15], and anti-GST antiserum was raised by immunizing a rabbit with purified GST protein. Other antibodies against NR1 (BD bioscience, Franklin Lakes, NJ, USA), NR2A/B (Invitrogen, Carlsbad, CA, USA), PSD-95 (Santa Cruz Biotechnology, Santa Cruz, CA, USA), β-adaptin (Santa Cruz), NCS1 (Biomol International, Exeter, UK) and actin (Abcam, Cambridge, UK) were commercially available. For immunoblotting, protein samples were resolved on sodium dodecyl sulfate (SDS)-polyacrylamide gels and transferred to PVDF membranes (Millipore, Bedford, MA, USA). The blots were blocked in Tris-buffered saline (TBS; 150 mM NaCl, 10 mM Tris, pH 7.6 and 2 mM $MgCl_2$) containing 0.1% Tween-20 and 5% BSA, and incubated with primary antibody at room temperature for 1 hr. All primary antibodies were used at 1:2000 of final dilutions. Immunoreactive bands were then probed with horseradish peroxidase-conjugated secondary antibody for 1 hr and developed using the ECL detection system (Thermo Fisher Scientific, Rockford, IL, USA). Optical densities of immunoreactive bands were quantified using NIH ImageJ software (downloaded from http://rsb.info.nih.gov/ij/), and then the relative amounts of target proteins were deduced by comparison with the optical band densities from serially diluted reference extracts.

Immunocytochemistry. Cultured hippocampal neurons at DIV16 were cotransfected with β-gal plus luciferase-RNAi or hippocalcin-RNAi, as indicated (1:4 ratio) with lipofectaime 2000. Three days later (DIV19), cells were fixed and double-stained for hippocalcin and PSD-95 and β-gal. Immunofluorescence images were acquired with a LSM510 confocal microscope (Carl Zeiss, Germany).

Surface expression of NMDA receptors. Biotinylation experiment for monitoring surface expression of the GluN1 NMDA receptor subunit was performed with a commercial surface labeling kit according to manufacturer's instructions (Thermo Fisher Scientific). Briefly, 400-μm-thick hippocampal slices (6-10 slices for each lane) were incubated with aCSF containing 1 mg/ml sulfosuccinimidyl-6-(biotinamido) hexanoate for 45 min on ice, quenched by further incubation in aCSF containing 100 mM glycine, and followed by two washes with ice-cold TBS (50 mM Tris, pH 7.6, 150 mM NaCl). Crude cell lysates were prepared in modified RIPA buffer containing 50 mM Tris (pH 7.6), 150 mM NaCl, 0.5% Triton X-100, 0.5% sodium deoxycholate, 0.1% SDS, 5 mM NaF, 1 mM Na_3VO_4 and protease inhibitor cocktail (Sigma). Small aliquots of each lysate were kept for total GluN1 protein levels. The detergent-solubilized lysates were incubated with 50 μl of hydrated Neutravidin-Agarose beads for 2 hr at 4°C to isolate biotinylated proteins. After the Neutravidin beads were washed

four times with the RIPA buffer, bound proteins were eluted with SDS sample buffer by boiling for 5 min. Isolated surface proteins and whole cell lysates were subsequently analyzed by immunoblotting with anti-GluN1 antibody. Equal loading of isolated surface proteins was confirmed based on silver-stained bands profiles on gels that were pre-run with small aliquots of samples.

***Co-immunoprecipitation*.** Crude lysates from hippocampal slices were prepared in modified RIPA buffer containing 50 mM Tris (pH 7.6), 150 mM NaCl, 0.5% Triton X-100, 5 mM NaF, 1 mM Na_3VO_4 and protease inhibitor cocktail, and then pre-cleared with Protein G-Sepharose beads (Millipore, Billerica, MA, USA) for 1 hr at 4°C. Two mg aliquots of pre-cleared lysates were subjected to immunoprecipitation with 5 μg of indicated antibodies for 4 hr at 4°C, and immunocomplexes were isolated by further incubation with 50 μl of hydrated Protein G-Sepharose beads for 2 hr at 4°C. The immunoprecipitates were washed four times with the RIPA buffer, and eluted by boiling in SDS sample buffer. Elutes were then subjected to immunoblotting. Optical densities of immunoreactive bands were quantified using NIH ImageJ software and normalized with those from the primary target of the immunoprecipitation in each lane.

***Mammalian two-hybrid assay*.** To examine whether hippocalcin can directly interact with NR1 or PSD95, we employed mammalian two-hybrid assay system as previously described with modifications[32]. DNA fragments corresponding to the indicated regions were amplified by RT-PCR, and cloned into pGEM-T vector (Promega, Madison, WI, USA). After confirming the sequence identities, the inserts were subcloned into pM or pVP16 vector for mammalian two-hybrid assay (BD bioscience; Supplement 2A). Expression of AD-or BD-tagged proteins was confirmed by immnoblotting with anti-AD and BD antibodies. pUAS-Luc (BD bioscience) was used as a reporter, and pRL-TK (Promega) as an internal control. Effector plasmids (400 ng each per well) were co-transfected with pUAS-Luc (20 ng per well) and pRL-TK (100 ng per well) into COS7 cells using Lipofectamine PLUS reagents (Invitrogen) in a 12-well plate scale. Luciferase assay was performed with a commercial kit (Promega) after 48 hr of transfection. Primer sequences used for cloning are as follows: NR1CT E1 up: 5'-GAA TTC GTA GCT GGG ATT TTC CTC A-3'; NR1CT H3 dn: 5'-AAG CTT CTC TCC CTA TGA CGG GAA CA-3'; 95PDZ E1 up: 5'-GAA TTC ATT GTC AAC ACG GAC ACC CTA-3'; 95PDZ H3 dn: 5'-AAG CTT CAT GAG CTG TTC CCG AAG AT-3'; 95S-G E1 up: 5'-GAA TTC AGG GCC CTG TTT GAT TAC G-3'; 95S-G H3 dn: 5'-AAG CTT CAG ATG TAG GGG CCT GAG AG-3'; HIP_{2-72} E1 up: 5'-GAA TTC GGC AAG

CAG AAT AGC AAG CTG-3'; HIP_{2-72} H3 dn: 5'-AAG CTT AAA AGT GCG GAA GAC ATG C-3'; $HIP_{104-192}$ E1 up: 5'-GAA TTC GCC TTC AGC ATG TAC GAC CT-3'; $HIP_{104-192}$ H3 dn: 5'-AAG CTT ACT AAC GGC TGC CTT GCT TA-3'.

***Glutathione-S-transferase (GST) pull-down assay*.** COS-7 cells ($5x10^7$) were transfected with AD-tagged NR1CT, 95PDZ or 95S-G expression plasmid. After 48 hr of transfection, cell lysates were prepared in modified RIPA buffer containing 50 mM Tris (pH 7.6), 150 mM NaCl, 0.5% Triton X-100, 0.5% sodium deoxycholate, 5 mM NaF, 1 mM Na_3VO_4 and protease inhibitor cocktail. Small aliquots of lysates were kept as an input. The solubilized proteins (1 mg each) were incubated with purified GST (300 ng) or GST-$Hippocalcin_{2-72}$ protein (100 ng) for 2 hr at 4°C. Protein complexes were then purified with a commercial GST purification kit according to the manufacturer's instructions (Millipore), and analyzed by immunoblotting.

REFERENCES

1. Collingridge, G.L., Kehi, S.J. & McLennan, H. Excitatory amino acids in synaptic transmission in the Schaffer collateral-commissural pathway of the rat hippocampus. *J. Physiol.* **334**, 33-46 (1983).
2. Morris, R.G., Anderson, E., Lynch, G.S. & Baudry, M. Selective impairment of learning and blockade of long-term potentiation by an N-methyl-D-aspartate receptor antagonist, AP5. *Nature* **319**, 774-776 (1986).
3. Bliss, T.V. & Collingridge, G.L. A synaptic model of memory: long-term potentiation in the hippocampus. *Nature* **361**, 31-39 (1993).

4 Fujii, S., Saito, K., Miyakawa, H., Ito, K. & Kato, H. Reversal of long-term potentiation (depotentiation) induced by tetanus stimulation of the input to CA1 neurons of guinea pig hippocampal slices. *Brain Res.* **555**, 112-122 (1991).

5. Dudek, S.M. & Bear, M.F. Homosynaptic long-term depression in area CA1 of hippocampus and effects of N-methyl-D-aspartate receptor blockade. *Proc. Natl. Acad. Sci. USA* **89**, 4363-4367 (1992).
6. Mulkey, R.M. & Malenka, R.C. Mechanisms underlying induction of homosynaptic long-term depression in area CA1 of the hippocampus. *Neuron* **9**, 967-975 (1992).
7. Collingridge, G.L., Peineau, S., Howland, J.G. & Wang, Y.T. Long-term depression in the CNS. *Nat. Rev. Neurosci.* **11**, 459-473 (2010).
8. Bashir, Z.I., Alford, S., Davies, S.N., Randall, A.D. & Collingridge, G.L. Long-term potentiation of NMDA receptor-mediated synaptic transmission in the hippocampus. *Nature* **349**, 156-158 (1991).
9. Abraham, W.C. & Bear, M.F. Metaplasticity: the plasticity of synaptic plasticity. *Trends Neurosci.* **19**, 126-130 (1996).
10. Collingridge, G.L., Isaac, J.T. & Wang, Y.T. Receptor trafficking and synaptic plasticity. *Nat. Rev. Neurosci.* **5**, 952-962 (2004).
11. Mulkey, R.M., Herron, C.E. & Malenka, R.C. An essential role for protein phosphatases in hippocampal long-term depression. *Science* **261**, 1051-1055 (1993).
12. Mulkey, R.M., Endo, S., Shenolikar, S. & Malenka, R.C. Involvement of a calcineurin/inhibitor-1 phosphatase cascade in hippocampal long-term depression. *Nature* **369**, 486-488 (1994).
13. Peineau, S. *et al.* LTP inhibits LTD in the hippocampus via regulation of GSK3beta. *Neuron* **53**, 703-717 (2007).

14. Peineau, S. *et al.* A systematic investigation of the protein kinases involved in NMDA receptor-dependent LTD: evidence for a role of GSK-3 but not other serine/threonine kinases. *Mol. Brain* **2**, 22 (2009).

15. Palmer, C.L. *et al.* Hippocalcin functions as a calcium sensor in hippocampal LTD. *Neuron* **47**, 487-494 (2005).

16. Kim, M.J. *et al.* Synaptic accumulation of PSD-95 and synaptic function regulated by phosphorylation of serine-295 of PSD-95. *Neuron* **56**, 488-502 (2007).

17. Xu, W. *et al.* Molecular dissociation of the role of PSD-95 in regulating synaptic strength and LTD. *Neuron* **57**, 248-262 (2008).

18. Harvey, J., Balasubramaniam, R. & Collingridge, G.L. Carbachol can potentiate N-methyl-D-aspartate responses in the rat hippocampus by a staurosporine and thapsigargin-insensitive mechanism. *Neurosci. Lett.* **162**, 165-168 (1993).

19. Markram, H. & Segal, M. Acetylcholine potentiates responses to N-methyl-D-aspartate in the rat hippocampus. *Neurosci. Lett.* **113**, 62-65 (1990).

20. Shinoe, T., Matsui, M., Taketo, M.M. & Manabe, T. Modulation of synaptic plasticity by physiological activation of M1 muscarinic acetylcholine receptors in the mouse hippocampus. *J. Neurosci.* **25**, 11194-11200 (2005).

21. Kirkwood, A., Rozas, C., Kirkwood, J., Perez, F. & Bear, M.F. Modulation of long-term synaptic depression in visual cortex by acetylcholine and norepinephrine. *J. Neurosci.* **19**, 1599-1609 (1999).

22. Dickinson, B.A. *et al.* A novel mechanism of hippocampal LTD involving muscarinic receptor-triggered interactions between AMPARs, GRIP and liprin-α. *Mol. Brain* **2**,18 (2009).

23. Jo, J. *et al.* Experience-dependent modification of mechanisms of long-term depression. *Nat. Neurosci.* **9**, 170-172 (2006).

24. Aramakis, V.B., Bandrowski, A.E. & Ashe, J.H. Role of muscarinic receptors, G-proteins, and intracellular messengers in muscarinic modulation of NMDA receptor-mediated synaptic transmission. *Synapse* **32**, 262-275 (1999).

25. Jo, J. *et al.* Metabotropic glutamate receptor-mediated LTD involves two interacting Ca^{2+} sensors, NCS-1 and PICK1. *Neuron* **60**, 1095-1111 (2008).

26. Volk, L.J., Pfeiffer, B.E., Gibson, J.R. & Huber, K.M. Multiple Gq-coupled receptors converge on a common protein synthesis-dependent long-term depression that is affected in fragile X syndrome mental retardation. *J. Neurosci.* **27**, 11624-11634 (2007).

27. Harney, S.C., Rowan, M. & Anwyl, R. Long-term depression of NMDA receptor-mediated synaptic transmission is dependent on activation of metabotropic glutamate

receptors and is altered to long-term potentiation by low intracellular calcium buffering. *J. Neurosci.* **26**, 1128-1132 (2006).

28. Ireland, D.R. & Abraham, W.C. Mechanisms of group I mGluR-dependent long-term depression of NMDA receptor-mediated transmission at Schaffer collateral-CA1 synapses. *J. Neurophysiol.* **101**, 1375-1385 (2009).
29. Burgoyne, R.D. Neuronal calcium sensor proteins: generating diversity in neuronal Ca^{2+} signalling. *Nat. Rev. Neurosci.* **8**, 182-193 (2007).
30. Roche, K.W. *et al.* Molecular determinants of NMDA receptor internalization. *Nat. Neurosci.* **4**, 794-802 (2001).
31. Hümmer, A. *et al.* Competitive and synergistic interactions of G protein β_2 and Ca^{2+} channel β_{1b} subunits with $Ca_v2.1$ channels, revealed by mammalian two-hybrid and fluorescence resonance energy transfer measurements. *J. Biol. Chem.* **278**, 49386-49400 (2003).
32. Nakagawa, T. *et al.* Quaternary structure, protein dynamics, and synaptic function of SAP97 controlled by L27 domain interactions. *Neuron* **44**, 453-467 (2004).
33. Lin, Y., Skeberdis, V.A., Francesconi, A., Bennett, M.V. & Zukin, R.S. Postsynaptic density protein-95 regulates NMDA channel gating and surface expression. *J. Neurosci.* **24**, 10138-10148 (2004).
34. Futai, K. *et al.* Retrograde modulation of presynaptic release probability through signaling mediated by PSD-95-neuroligin. *Nat. Neurosci.* **10**, 186-195 (2007).
35. Lau, C.G. & Zukin, R.S. NMDA receptor trafficking in synaptic plasticity and neuropsychiatric disorders. *Nat. Rev. Neurosci.* **8**, 413-426 (2007).
36. Tzingounis, A.V., Kobayashi, M., Takamatsu, K. & Nicoll, R.A. Hippocalcin gates the calcium activation of the slow afterhyperpolarization in hippocampal pyramidal cells. *Neuron* **53**, 487-493 (2007).
37. Holbro, N., Grunditz, A. & Oertner, T.G. Differential distribution of endoplasmic reticulum controls metabotropic signaling and plasticity at hippocampal synapses. *Proc. Natl. Acad. Sci. USA* **106**, 15055-15060 (2009).
38. Carroll, R.C. *et al.* Dynamin-dependent endocytosis of ionotropic glutamate receptors. *Proc. Natl. Acad. Sci. USA* **96**, 14112-14117 (1999).
39. Migaud, M. *et al.* Enhanced long-term potentiation and impaired learning in mice with mutant postsynaptic density-95 protein. *Nature* **396**, 433-439 (1998).
40. Bhattacharyya, S., Biou, V., Xu, W., Schlüter, O. & Malenka, R.C. A critical role for PSD-95/AKAP interactions in endocytosis of synaptic AMPA receptors. *Nat. Neurosci.* **12**, 172-181 (2009).

41. Ehrlich, I., Klein, M., Rumpel, S. & Malinow, R. PSD-95 is required for activity-driven synapse stabilization. *Proc. Natl. Acad. Sci. USA* **104**, 4176-4181 (2007).
42. Elias, G.M., Elias, L.A., Apostolides, P.F., Kriegstein, A.R. & Nicoll, R.A. Differential trafficking of AMPA and NMDA receptors by SAP102 and PSD-95 underlies synapse development. *Proc. Natl. Acad. Sci. USA* **105**, 20953-20958 (2008).
43. Anderson, W.W. & Collingridge, G.L. The LTP Program: a data acquisition program for on-line analysis of long-term potentiation and other synaptic events. *J. Neurosci. Methods* **108**, 71-83 (2001).
44. Brummelkamp, T.R., Bernards, R. & Agami, R. A system for stable expression of short interfering RNAs in mammalian cells. *Science* **296**, 550-553 (2002).

Figure 1

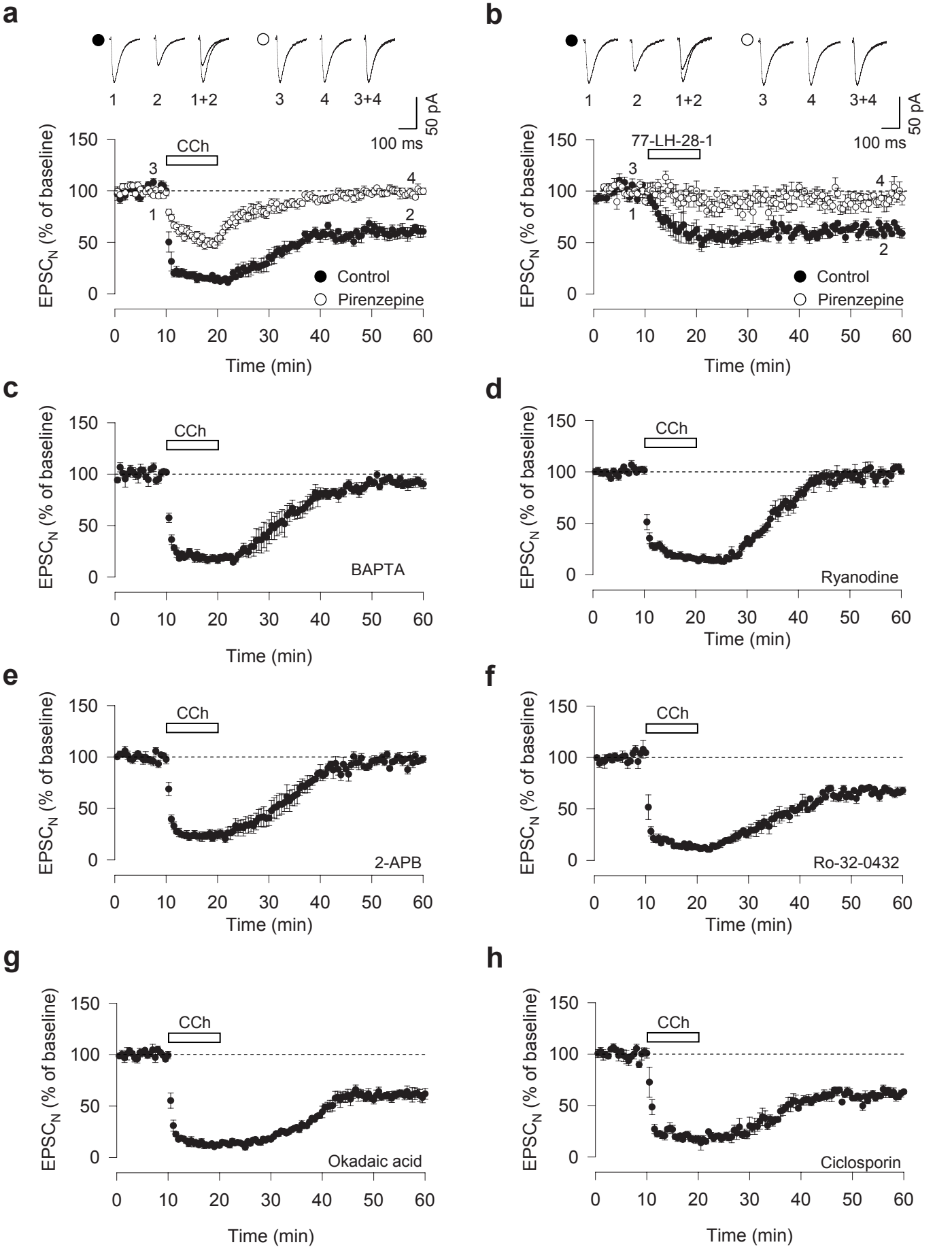
a
b
1
2
1+2
3
4
3+4
50 pA
100 ms
CCh
77-LH-28-1
EPSC$_N$ (% of baseline)
Control
Pirenzepine
Time (min)
c
BAPTA
d
Ryanodine
e
2-APB
f
Ro-32-0432
g
Okadaic acid
h
Ciclosporin

Figure 2

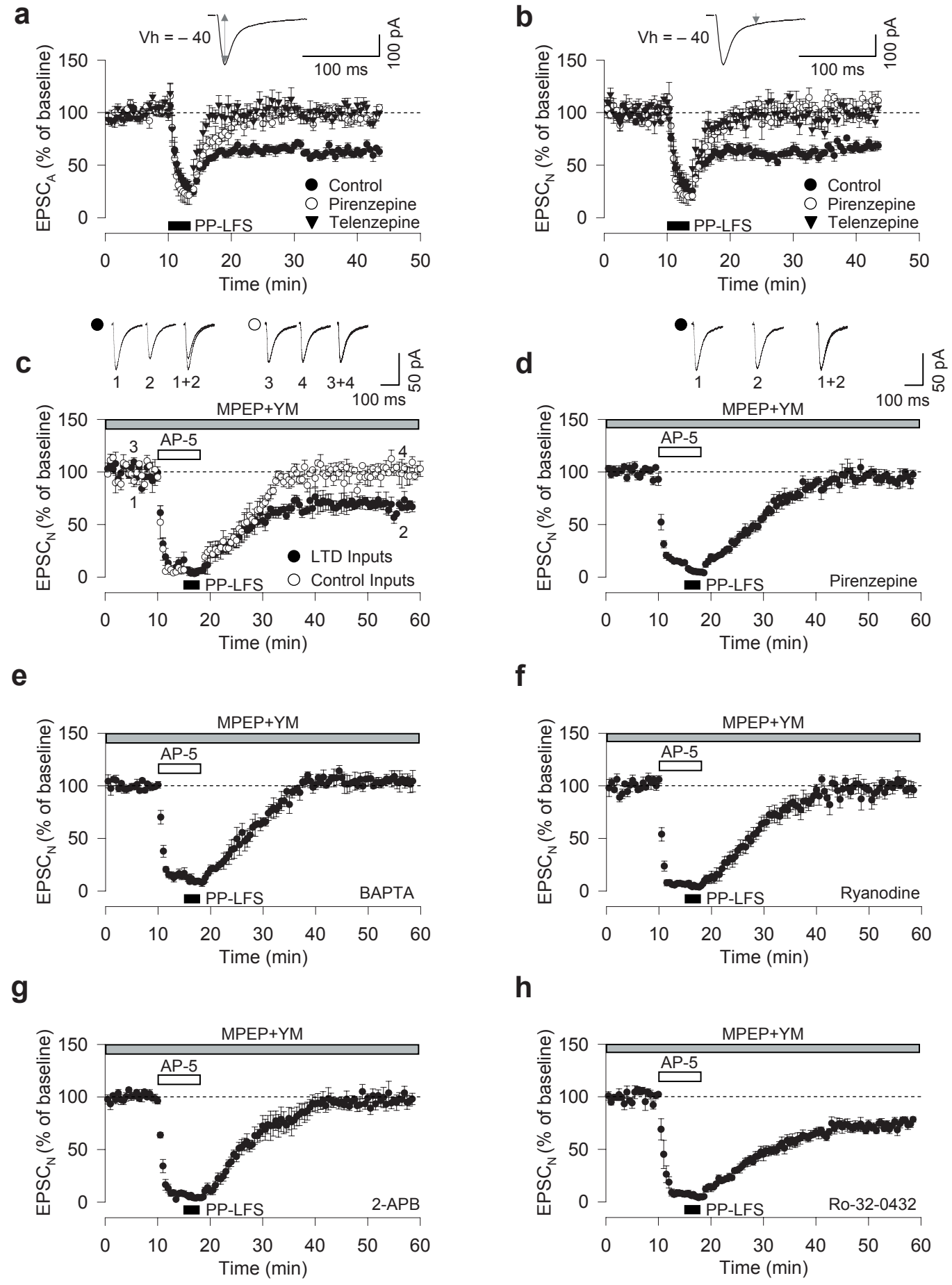
a
Vh = – 40
100 pA
100 ms
EPSC$_A$ (% of baseline)
Control
Pirenzepine
Telenzepine
PP-LFS
Time (min)
b
Vh = – 40
100 pA
100 ms
EPSC$_N$ (% of baseline)
Control
Pirenzepine
Telenzepine
PP-LFS
Time (min)
c
1
2
1+2
3
4
3+4
50 pA
100 ms
MPEP+YM
AP-5
EPSC$_N$ (% of baseline)
LTD Inputs
Control Inputs
PP-LFS
Time (min)
d
1
2
1+2
50 pA
100 ms
MPEP+YM
AP-5
EPSC$_N$ (% of baseline)
PP-LFS
Pirenzepine
Time (min)
e
MPEP+YM
AP-5
EPSC$_N$ (% of baseline)
PP-LFS
BAPTA
Time (min)
f
MPEP+YM
AP-5
EPSC$_N$ (% of baseline)
PP-LFS
Ryanodine
Time (min)
g
MPEP+YM
AP-5
EPSC$_N$ (% of baseline)
PP-LFS
2-APB
Time (min)
h
MPEP+YM
AP-5
EPSC$_N$ (% of baseline)
PP-LFS
Ro-32-0432
Time (min)

Figure 3

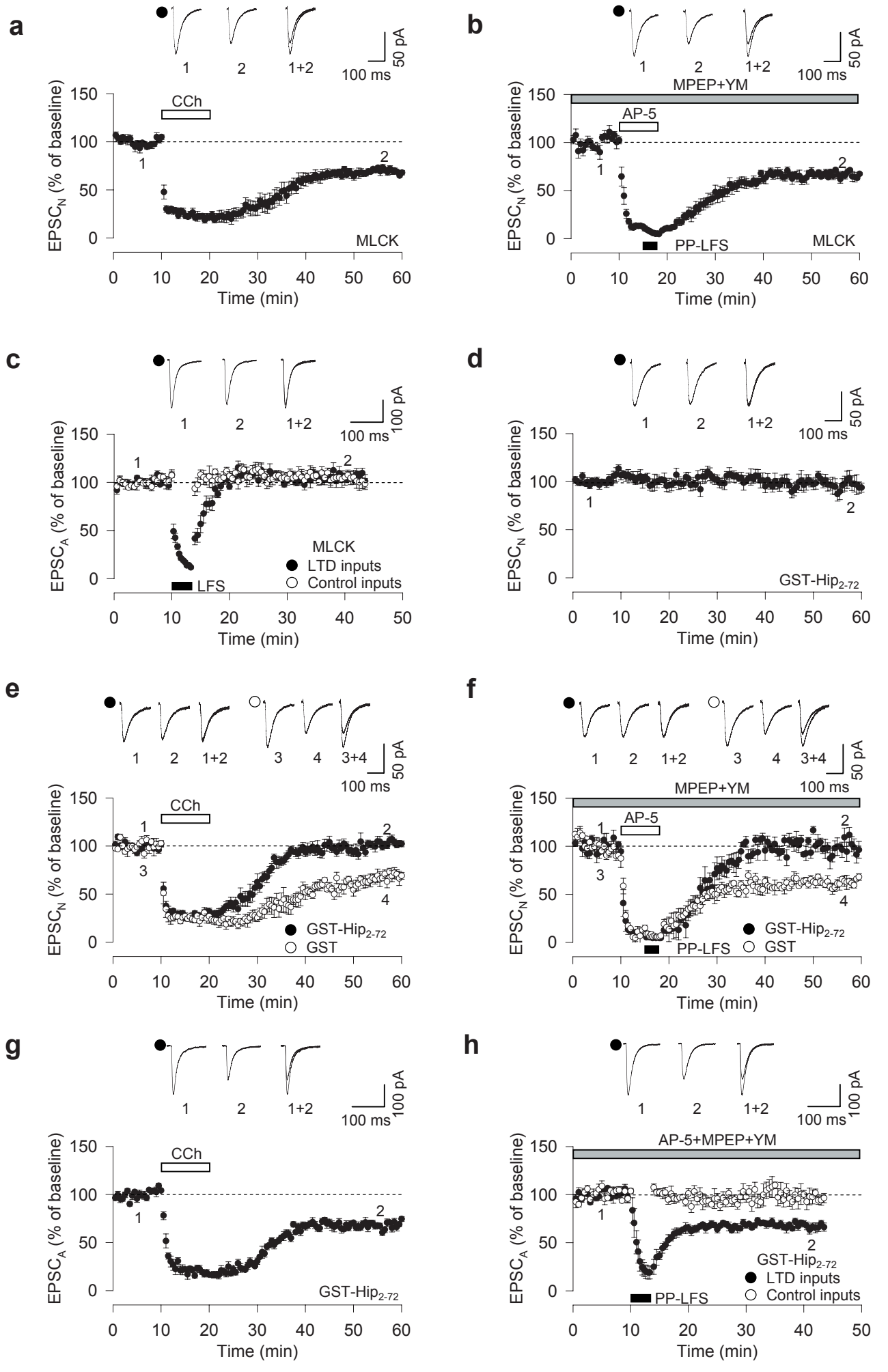
a
b
c
d
e
f
g
h
CCh
MPEP+YM
AP-5
AP-5+MPEP+YM
PP-LFS
LFS
MLCK
GST-Hip2-72
GST
LTD inputs
Control inputs
EPSCN (% of baseline)
EPSCA (% of baseline)
Time (min)
50 pA
100 pA
100 ms
1
2
1+2
3
4
3+4

Figure 4

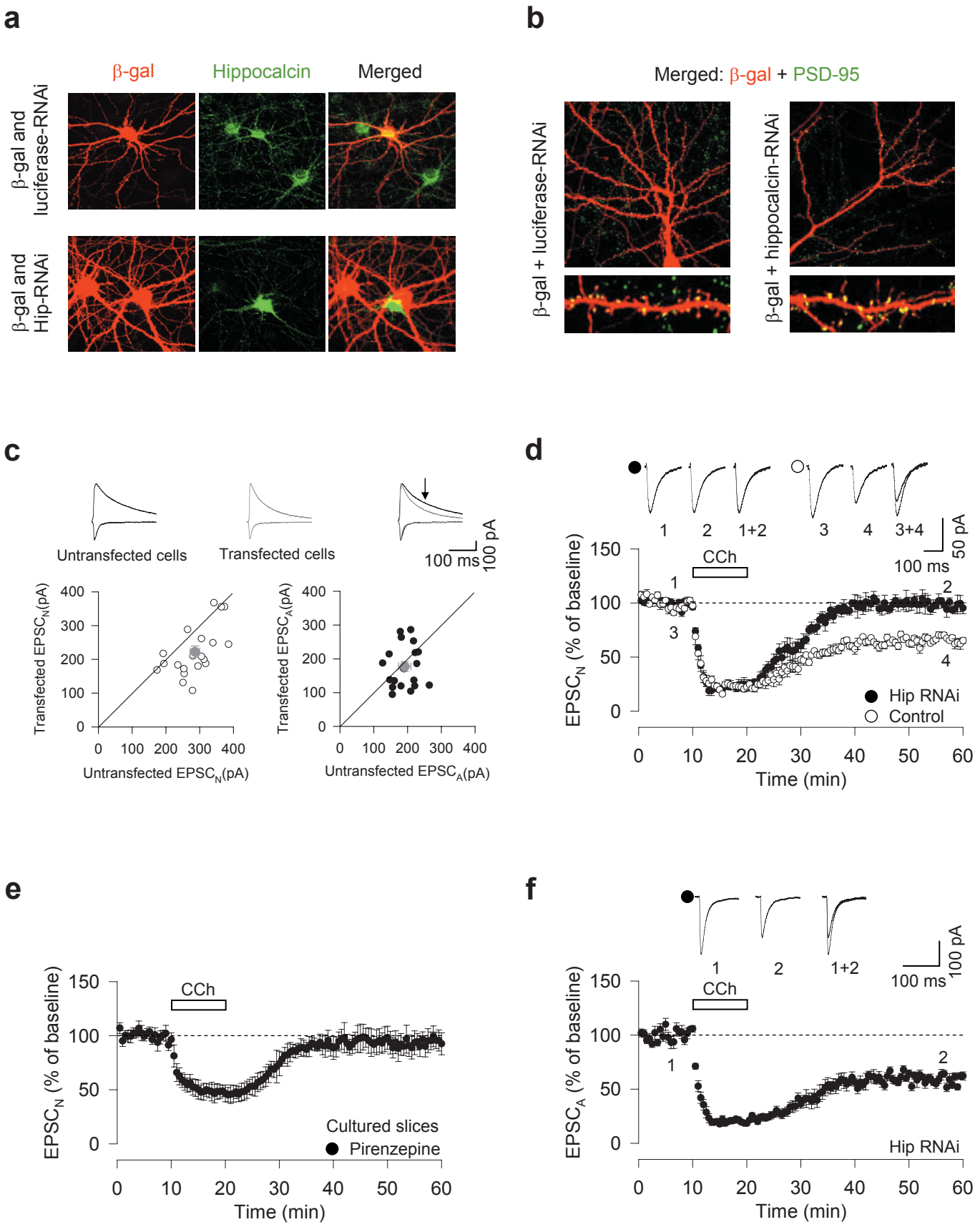
a
β-gal
Hippocalcin
Merged
β-gal and luciferase-RNAi
β-gal and Hip-RNAi
b
Merged: β-gal + PSD-95
β-gal + luciferase-RNAi
β-gal + hippocalcin-RNAi
c
Untransfected cells
Transfected cells
100 ms
100 pA
Transfected EPSC$_N$(pA)
Untransfected EPSC$_N$(pA)
Transfected EPSC$_A$(pA)
Untransfected EPSC$_A$(pA)
d
1
2
1+2
3
4
3+4
50 pA
100 ms
CCh
EPSC$_N$ (% of baseline)
Hip RNAi
Control
Time (min)
e
CCh
EPSC$_N$ (% of baseline)
Cultured slices
Pirenzepine
Time (min)
f
1
2
1+2
100 pA
100 ms
CCh
EPSC$_A$ (% of baseline)
Hip RNAi
Time (min)

Figure 5

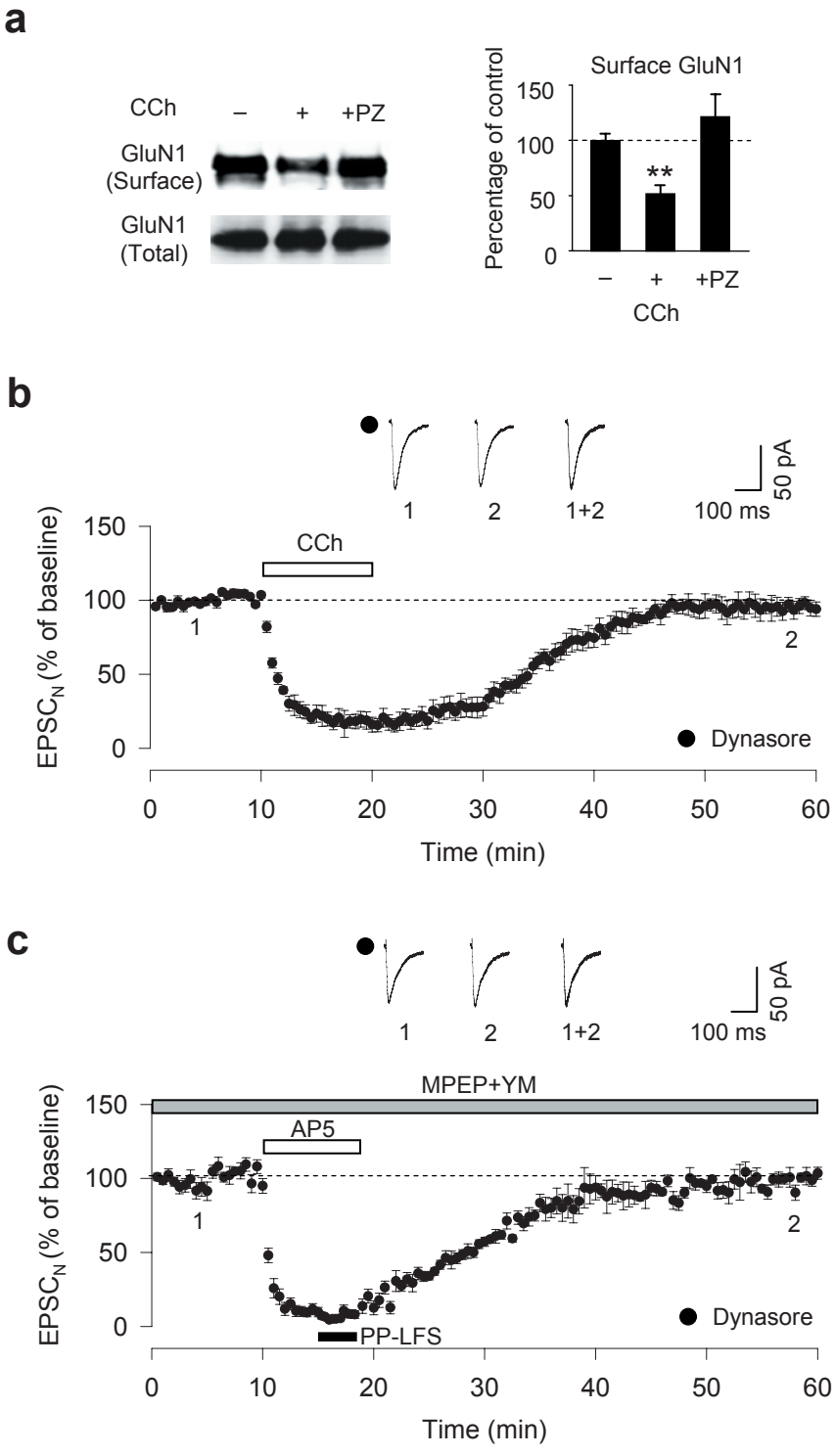
a
CCh
–
+
+PZ
GluN1
(Surface)
GluN1
(Total)
Surface GluN1
Percentage of control
150
100
50
0
**
–
+
+PZ
CCh
b
1
2
1+2
100 ms
50 pA
CCh
EPSC$_N$ (% of baseline)
Dynasore
Time (min)
c
MPEP+YM
AP5
PP-LFS

Figure 6

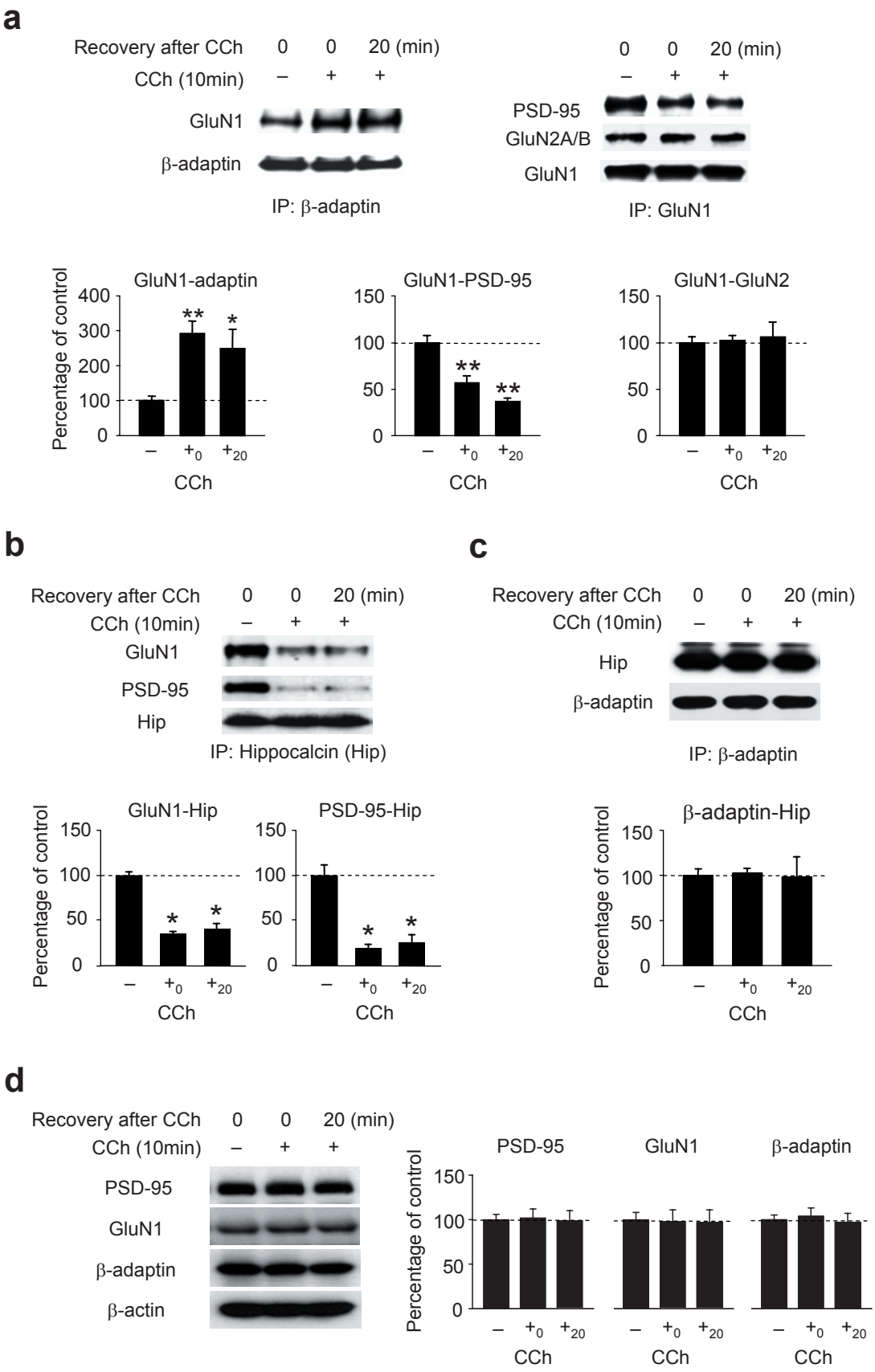
a
Recovery after CCh 0 0 20 (min)
CCh (10min) – + +
GluN1
β-adaptin
IP: β-adaptin
PSD-95
GluN2A/B
GluN1
IP: GluN1
GluN1-adaptin
GluN1-PSD-95
GluN1-GluN2
Percentage of control
CCh
b
Hip
IP: Hippocalcin (Hip)
GluN1-Hip
PSD-95-Hip
c
β-adaptin
IP: β-adaptin
β-adaptin-Hip
d
PSD-95
β-actin

Figure 7

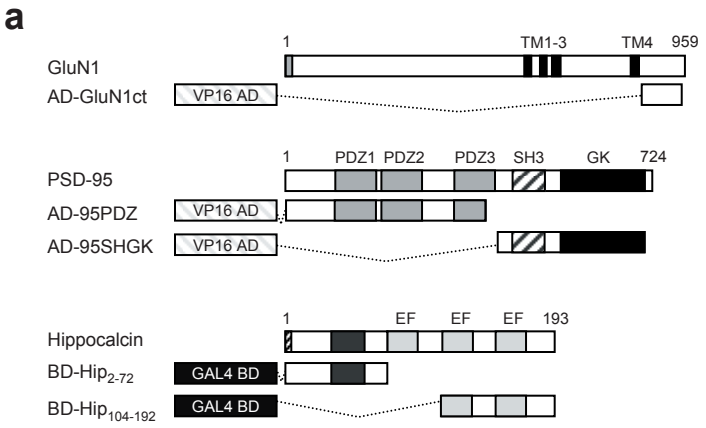

b

AD \ BD	Empty	Hip_{2-72}	$Hip_{104-192}$
GluN1ct	–	–	–
95PDZ	–	+	–
95SHGK	–	+++	–

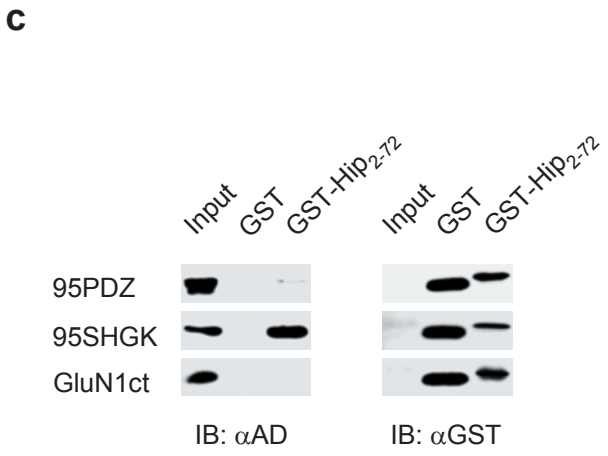

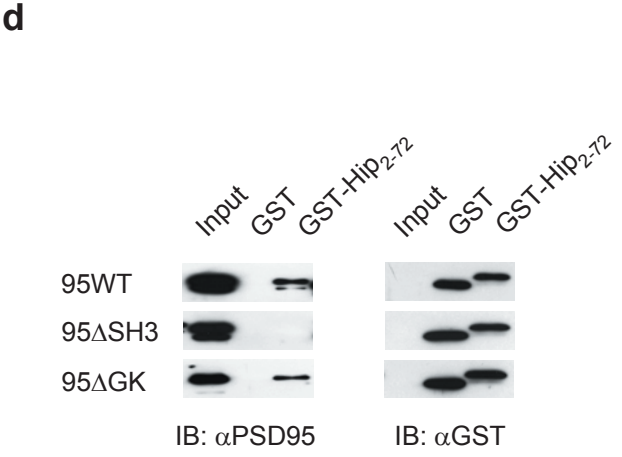

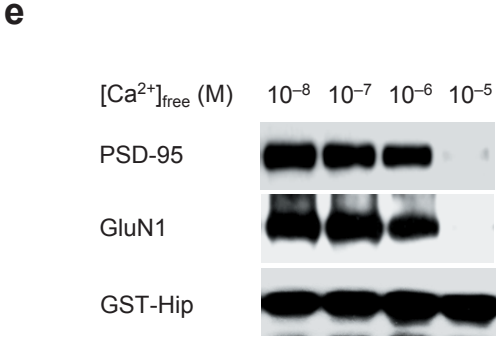

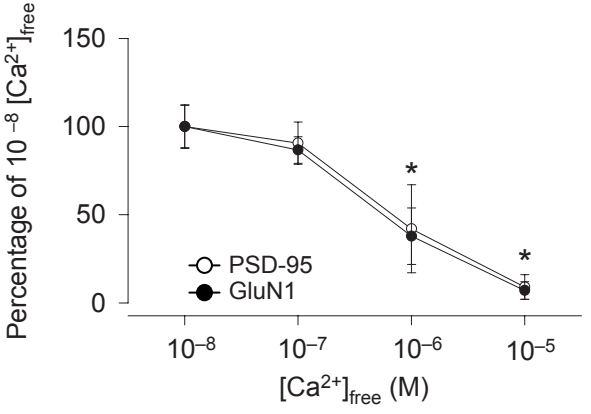

Figure 8

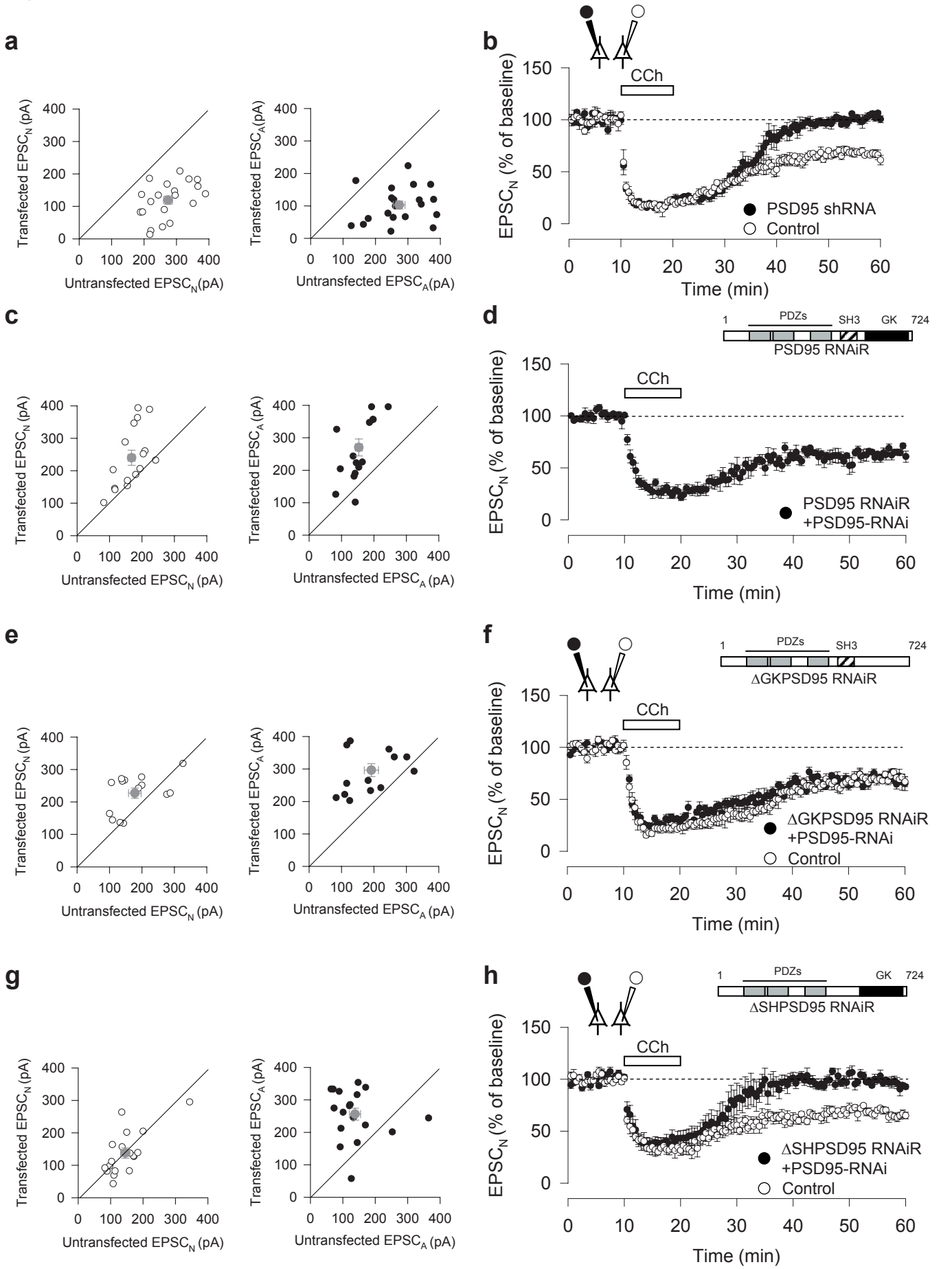
a
Transfected EPSC$_N$ (pA)
Untransfected EPSC$_N$(pA)
Transfected EPSC$_A$(pA)
Untransfected EPSC$_A$(pA)
b
CCh
PSD95 shRNA
Control
EPSC$_N$ (% of baseline)
Time (min)
c
d
PDZs
SH3
GK
724
PSD95 RNAiR
PSD95 RNAiR
+PSD95-RNAi
e
f
ΔGKPSD95 RNAiR
ΔGKPSD95 RNAiR
+PSD95-RNAi
g
h
ΔSHPSD95 RNAiR
ΔSHPSD95 RNAiR
+PSD95-RNAi

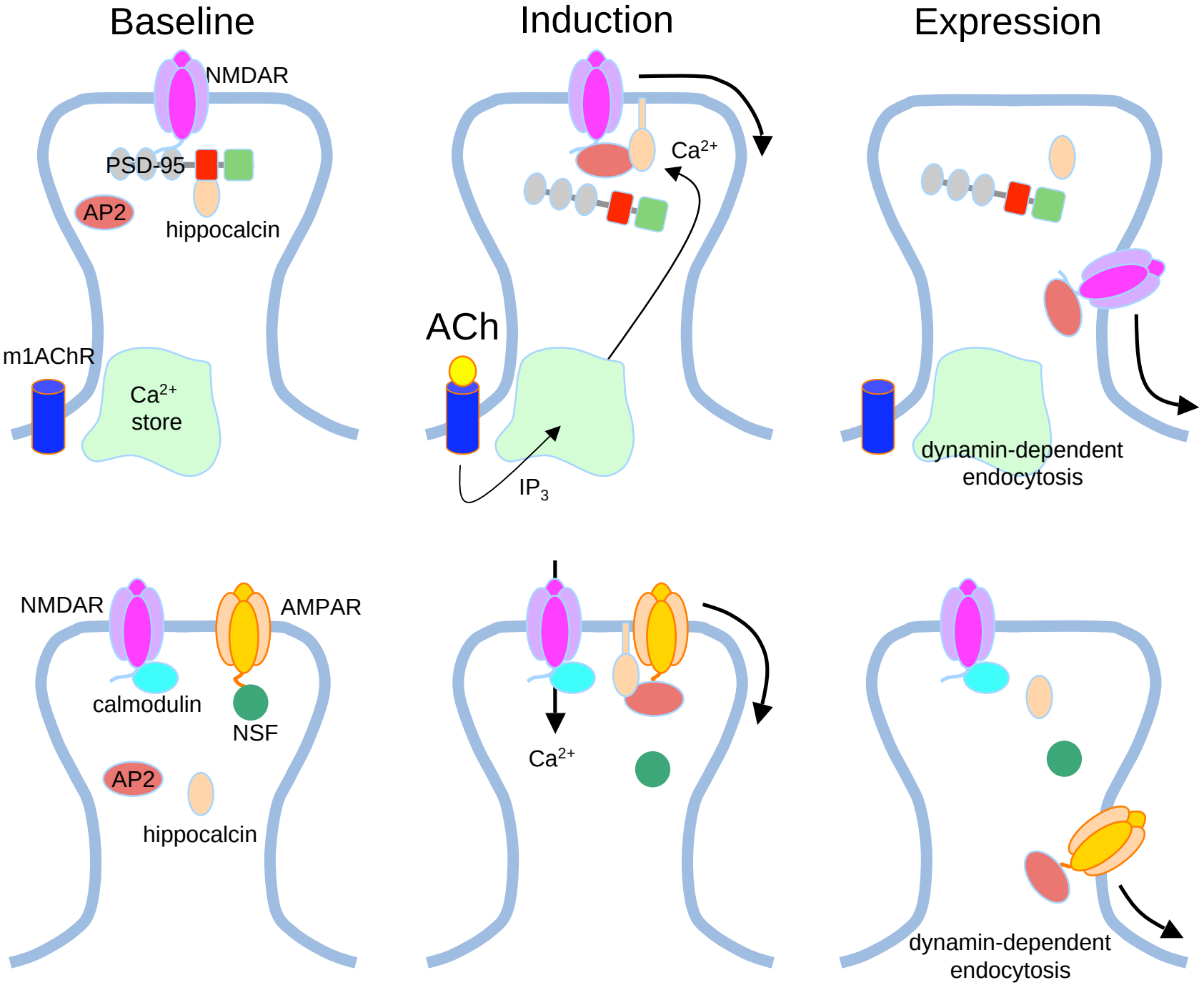
Baseline
Induction
Expression
NMDAR
PSD-95
AP2
hippocalcin
m1AChR
Ca2+ store
ACh
Ca2+
IP3
dynamin-dependent endocytosis
NMDAR
AMPAR
calmodulin
NSF
AP2
hippocalcin
Ca2+
dynamin-dependent endocytosis

Supplementary Figure Legend.

A possible scheme to explain the role of hippocalcin in (top) mAChR-LTD_N and (bottom) NMDAR-LTD_A. It is postulated that mAChR-LTD_N operates in a subset of spines, which contain the machinery required for IP_3-mediated release of Ca^{2+} from intracellular stores. Hippocalcin is bound to the SH3 region of PSD-95, which in turn binds the GluN2 subunit of NMDARs to prevent the binding of the β-adaptin subunit of AP2. On sensing an increase in Ca^{2+} hippocalcin translocates to the plasma membrane and this permits the dissociation of PSD-95 from the NMDAR by an unknown mechanism. NMDARs are then able to bind AP2, which initiates their dynamin- and clathrin-dependent endocytosis. In contrast, for NMDAR-LTD_A the process is initiated by Ca^{2+} entry through NMDARs. Ca^{2+} causes translocation of hippocalcin to the plasma membrane and this targets AP2 to the proximity of the GluA2 subunit of the AMPAR. This in turn enables AP2 to exchange for NSF and initiate the removal of AMPARs from the synapse, by lateral diffusion followed by clathrin-mediated endocytosis.